


RESEARCH ARTICLE

Open Access



PbrSLAH3 is a nitrate-selective anion channel which is modulated by calcium-dependent protein kinase 32 in pear

Guodong Chen[†], Li Wang[†], Qian Chen, Kaijie Qi, Hao Yin, Peng Cao, Chao Tang, Xiao Wu, Shaoling Zhang, Peng Wang* and Juyou Wu* 

Abstract

Background: The functional characteristics of *SLAC/SLAH* family members isolated from *Arabidopsis thaliana*, poplar, barley and rice have been comprehensively investigated. However, there are no reports regarding *SLAC/SLAH* family genes from *Rosaceae* plants.

Results: In this study, the function of PbrSLAH3, which is predominately expressed in pear (*Pyrus bretschneideri*) root, was investigated. PbrSLAH3 can rescue the ammonium toxicity phenomenon of *slah3* mutant plants under high-ammonium/low-nitrate conditions. In addition, yeast two-hybrid and bimolecular fluorescence complementation assays confirmed that PbrSLAH3 interacts with PbrCPK32. Moreover, when *PbrSLAH3* was co-expressed with either the *Arabidopsis* calcium-dependent protein kinase (*CPK*) 21 or *PbrCPK32* in *Xenopus* oocytes, yellow fluorescence was emitted from the oocytes and typical anion currents were recorded in the presence of extracellular NO_3^- . However, when *PbrSLAH3* alone was injected, no yellow fluorescence or anion currents were recorded, suggesting that anion channel PbrSLAH3 activity was controlled through phosphorylation. Finally, electrophysiological and transgene results showed that PbrSLAH3 was more permeable to NO_3^- than Cl^- .

Conclusion: We suggest that PbrSLAH3 crossing-talk with PbrCPK32 probably participate in transporting of nitrate nutrition in pear root.

Keywords: Nitrogen, Signaling, Anion channel, Nitrate, PbrSLAH3, Phosphorylation

Background

Anion channels, which widely exist in a variety of bio-membranes, play an important role in cell signaling, osmoregulation, metabolism, stress tolerance and plant nutrition [1–4]. Electrophysiological data from different research groups confirmed that rapid-type (R-type) and slow-type (S-type) anion channels are involved in anion transport [5–7]. By far, *SLAC/SLAH* family genes (S-type anion channels) from species, including *Arabidopsis thaliana*, poplar, barley and rice, have been identified and studied, five members in *Arabidopsis* [8, 9], seven members in *Populus* [10] and nine members in rice [11].

However, no reports regarding *SLAC/SLAH* family genes from *Rosaceae* plants have been found.

To date, only the physiological functions of the *SLAC/SLAH* family members in *Arabidopsis* have been widely studied [12–15]. *AtSLAC1*, together with *SLAC1* homologous 3 (*AtSLAH3*), plays an important role in regulating ABA-induced stomatal closure [16–19]. During this process, ABA is firstly perceived by the RCAR/PYR/PYL–ABI1 complex, which then releases protein kinase from *ABI1*-induced inhibition, and then *AtSLAC1* and *AtSLAH3* are activated by the calcium-independent protein kinase OST1 and the calcium-dependent protein kinases (CPKs) of *Arabidopsis* [13]. Meanwhile, other members of the *SLAC/SLAH* family in *Arabidopsis* have also been intensively studied. The results from the Geiger group showed that *SLAH1*, as a silent subunit, facilitates *SLAH3*-mediated chloride efflux from pericycle

* Correspondence: wangpeng@njau.edu.cn; juyouwu@njau.edu.cn

[†]Guodong Chen and Li Wang contributed equally to this work. Center of Pear Engineering Technology Research, State Key Laboratory of Crop Genetics and Germplasm Enhancement, College of Horticulture, Nanjing Agricultural University, No. 6. Tongwei Road, Nanjing, China



cells into the root xylem vessels [20, 21]. When co-expression the silent *SLAH1* subunit and *SLAH3* in *Xenopus* oocytes, *SLAH3* was activated even in the absence of nitrate and calcium-dependent protein kinases [20]. Besides, *SLAH2*, another member of the *SLAC/SLAH* family, which is expressed in the stele of the root, acts in a nitrate-specific channel that is impermeable to chloride when co-expressed with protein kinases in *Xenopus* oocytes [22].

Although *AtSLAC1* and *AtSLAH3* exhibit similar physiological functions in guard cells, different expression patterns and functional characteristics were observed between these two channels. For instance, *AtSLAC1* is exclusively expressed in the guard cells [23], while *AtSLAH3*, in addition to being expressed in the guard cells, is also predominantly expressed in the root and weakly expressed in the pollen tube [24, 25]. Furthermore, *AtSLAC1* exhibits a high permeability to NO_3^- than Cl^- , with a $\text{P}(\text{NO}_3^-)/\text{P}(\text{Cl}^-)$ ratio of 10 [22], while *AtSLAH3* is a nitrate-activated S-type anion channel with a $\text{P}(\text{NO}_3^-)/\text{P}(\text{Cl}^-)$ ratio of 20 [13, 14]. Apart from regulating the stomatal closure together with *AtSLAC1*, *AtSLAH3* alleviates ammonium toxicity and regulates pollen tube growth in *Arabidopsis* [25].

More importantly, *SLAC/SLAH* family genes from different plant species with high similarity showed varied expression patterns and functional characteristics. For instance, in contrast to *AtSLAC1*, which is permeable to both chloride and nitrate, *OsSLAC1* is identified as a nitrate-selective anion channel [11]. Furthermore, in contrast to *AtSLAH3*, which is predominantly expressed in the root and is dependent on phosphorylation activation, *PttSLAH3*, which is predominantly expressed in poplar secretory epithelia, is independent of activation by protein kinases [10]. Thus, based on these results mentioned above, we speculated that *SLAH3* isolated from the pear, which has not been clarified until recently, may own special functional-characteristics.

Nitrate is the major source of nitrogen for plants in nature and in agriculture under aerobic conditions [14, 26, 27]. *SLAC/SLAH* genes from different species have been proven to play an important role in nitrate transport. In this study, we focused on investigating the function of *PbrSLAH3*, which is predominantly expressed in pear root verified by RT-PCR, qRT-PCR and β -Glucuronidase (GUS) staining assays. The physiological function of *PbrSLAH3* was investigated by its over-expression in a *slah3* mutant. In consistent with that of *AtSLAH3*, *PbrSLAH3* also participates in alleviation of ammonium toxicity under high ammonium/low nitrate conditions. Furthermore, both yeast two-hybrid and bimolecular fluorescence complementation (BiFC) assays confirmed the interaction between *PbrSLAH3* and *PbrCPK32*. Finally, an electrophysiological experiment

revealed that *PbrSLAH3* is activated by *PbrCPK32* and the channel is highly selective for nitrate without obvious permeability to chloride. Thus, we conclude that *PbrSLAH3* serve as a nitrate efflux channel and may participate in nitrate transport in pear root.

Results

The phylogeny and expression patterns of *SLAC/SLAH* genes in pear

AtSLAC/SLAH orthologous in pear were identified by a BLASTp algorithm-based search of the pear genomic database (<http://peargenome.njau.edu.cn/>) using the amino acid sequences of *AtSLAC/SLAH* as queries. To compare the similarity levels between the *PbrSLAC/SLAH* and *AtSLAC/SLAH*, a rooted phylogenetic tree was constructed using the neighbor-joining method (Fig. 1a). As shown in Fig. 1, *PbrSLAC1* and *AtSLAC1* were grouped to the same branch, while other three *PbrSLAC/SLAH* proteins, together with *AtSLAH2* and *AtSLAH3*, belonged to another branch. Orthologs of *AtSLAC/SLAH* in pear did not phylogenetically cluster with *AtSLAH1* and *AtSLAH4*. To further determine which genes in the *PbrSLAC/SLAH* family may participate in nitrate transporting in pear root, the expression patterns of *PbrSLAC/SLAH* family genes in the root, leaf, pollen grain and pollen tube were analyzed by quantitative and semi-quantitative RT-PCR (Fig. 1b and c). *PbrSLAC1* was exclusively expressed in leaf, while *PbrSLAH3*, *PbrSLAH2/3-2* and *PbrSLAH2/3-3* were widely expressed in root, leaf and pollen. *PbrSLAH3* displayed a relative higher expression level than the other *PbrSLAH2/3* genes in pear root (Fig. 1b). Furthermore, the transcriptome data analysis suggested that the expression level of *PbrSLAH3* was up-regulated during nitrate starvation and then, after the re-supply of nitrate, its expression level was gradually down-regulated (Additional file 1: Figure S1). Taken together these results, we presume that *PbrSLAH3* may be involved in nitrate transport in pear root and may play an important role in nitrate nutrition in pear trees.

Subcellular localization and accurate organizational positions of *PbrSLAH3*

To determine the subcellular localization of *PbrSLAH3*, the fusion gene of *PbrSLAH3*-GFP was constructed and transformed into tobacco (*N. benthamiana*) leaves. As previously reported, the control GFP was uniformly distributed throughout the whole cell, and the *PbrSLAH3*-GFP fusion protein was observed exclusively in the plasma membrane with a Zeiss LSM 780 Image Browser (Fig. 2a). To further identify the accurate expression profiles of *PbrSLAH3* in pear, transgenic *Arabidopsis* plants carrying a GUS gene under control of the *PbrSLAH3* promoter fragment (2000 bp) were generated. The GUS activity assays

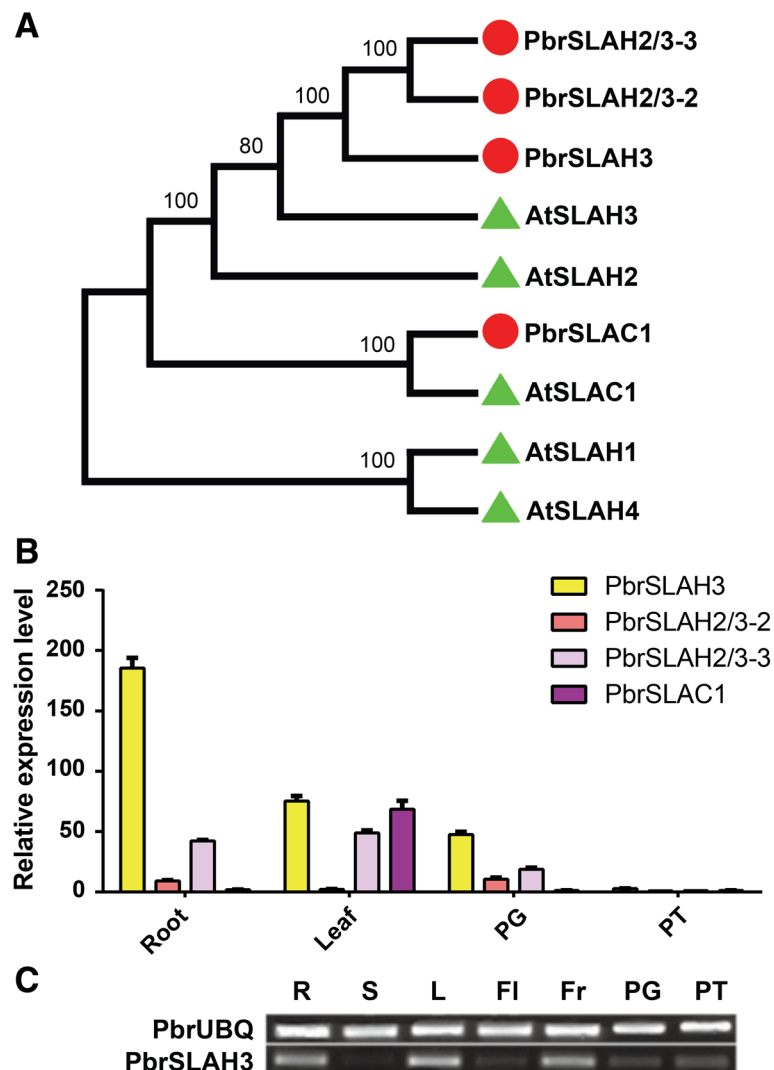


Fig. 1 The determination of S-type anion channels in pear and the expression analysis. **a** Phylogenetic tree of the *Arabidopsis thaliana* SLAC/SLAH anion channel family and the pear orthologs. Four putative PbrSLAC/SLAH anion channels were identified in the *Pyrus* genome database. *PbrSLAC1* appears to be related to *AtSLAC1*, other three homologs were classified into the *AtSLAH2/3* group, while *AtSLAH1/4* homologs could not be identified in pear. The *PbrSLAH2/3-1* sequence was used to clone the ortholog from *Pyrus bretschneideri* and named *PbrSLAH3*. **b** The expression patterns of *PbrSLAC/SLAH* family genes in the root, leaf, pollen grain and pollen tube of pear were analyzed by qRT-PCR. The values displayed in the figure were the geometric means of the relative expression of *PbrSLAC/SLAH* when both *PbrTUB* and *PbrUBQ* as reference genes. Three biological and three technical replicates were processed for the qRT-PCR assays. The error bars indicate standard deviations. The data are shown as mean values \pm SDs. **c** RT-PCR was used to confirm the expression patterns of the *PbrSLAH3* gene and *PbrUBQ* gene was used as an internal control

showed that *PbrSLAH3* is strongly expressed in roots, young leaves, mature leaves and stoma, and is weakly expressed in stems. However, it is not expressed in seed and silique (Fig. 2b-g). Thus, we presume that *PbrSLAH3* may have diverse functions similar to those of *AtSLAH3*, which plays an important role in the alleviation of ammonium toxicity and regulation of stomatal closure and pollen growth.

Functional characterization of *PbrSLAH3* in *Arabidopsis*

In line with previous reports, the *Arabidopsis slah3-3* mutant exhibited more severe ammonium toxicity than

wild-type when grown on plates containing a high-ammonium/low-nitrate medium [25]. As shown in Fig. 3a, the T-DNA insertion site in the *slah3-3* mutant was in the second intron of *AtSLAH3*. To examine the physiological function of *PbrSLAH3*, complementation lines of the *Arabidopsis slah3-3* mutant were constructed by the gene of *PbrSLAH3*. Two transgenic lines were selected based on the RT-PCR results. The mRNA of *PbrSLAH3* was not detected in wild-type and *slah3-3* mutant plants, but it was highly expressed in the transgenic lines (Fig. 3b). Phenotype testing showed that the ammonium

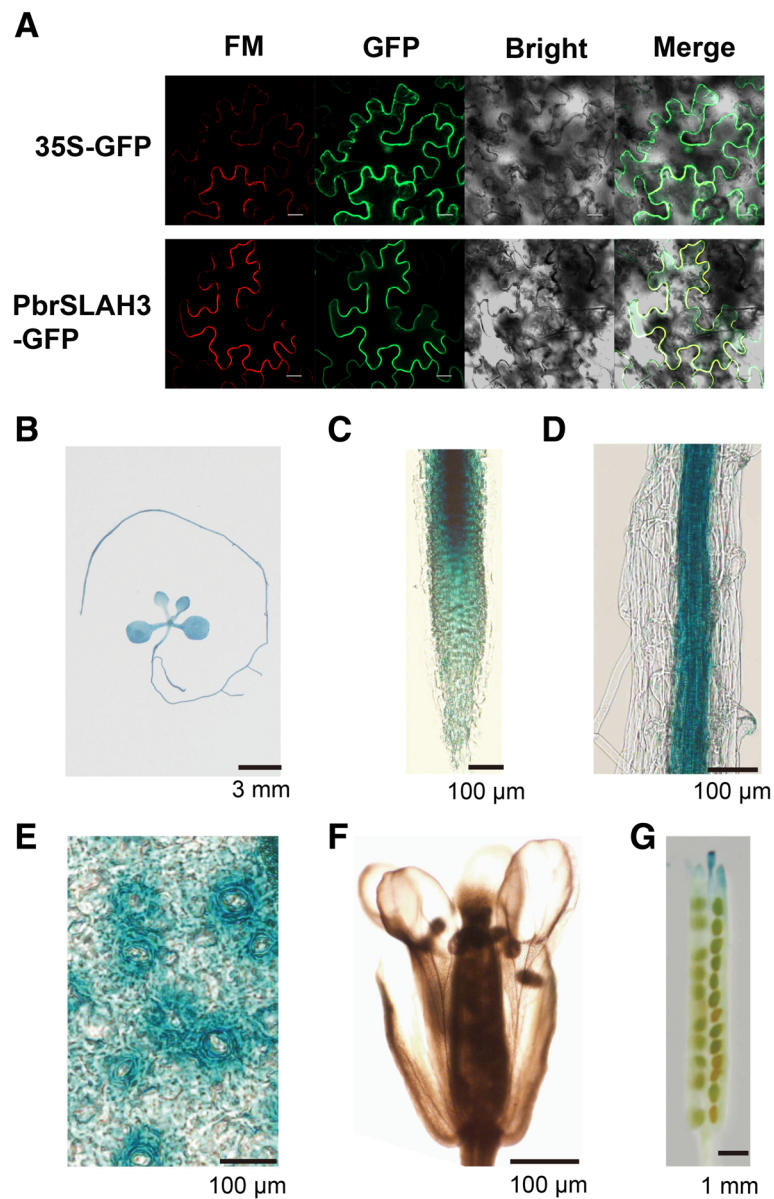


Fig. 2 The subcellular localization of *PbrSLAH3* to the plasma membrane, and a histochemical analysis of GUS activity in *PbrSLAH3* transgenic *Arabidopsis* (Col-0) plants. **a** GFP fluorescence emitted from the leaves of tobacco infected by *Agrobacterium* harboring *PbrSLAH3*-GFP was detected under a confocal microscope and the plasma membranes are stained red by FM4-64. GFP: green fluorescent protein; Chl: chlorophyll; Bright: bright-field image of *Agrobacterium tumefaciens*-infiltrated tobacco leaves; Merge: merged fluorescent images; Bar = 10 μ m. **b–g** GUS-histochemical analysis performed with *Arabidopsis* plants expressing the reporter gene under the control of the *PbrSLAH3* promoter. *PbrSLAH3* was expressed in young leaves, mature leaves, roots, stems, epidermal hairs, stomatal and siliques

toxicity phenotype of the *slah3-3* mutant under high-ammonium/low-nitrate conditions was rescued by the overexpression of *PbrSLAH3* (Fig. 3c and Additional file 1: Figure S2). Statistical results demonstrated that the root length of the *slah3-3* mutant was approximately 56–70% that of the wild-type when grown on high NH_4^+ medium supplied with 0 or 0.1 mM KNO_3 , while there were no differences between each of the

complementation lines and the wild-type (Fig. 3d–g), suggesting that *PbrSLAH3* plays an important role in the alleviation of ammonium toxicity under nitrate-limited conditions. Furthermore, when the KNO_3 concentration in the medium reaching up to 1 mM or more (20 mM), no clear differences were observed between the *slah3-3* mutant and wild-type, indicating that sufficient levels of nitrate can counteract ammonium toxicity.

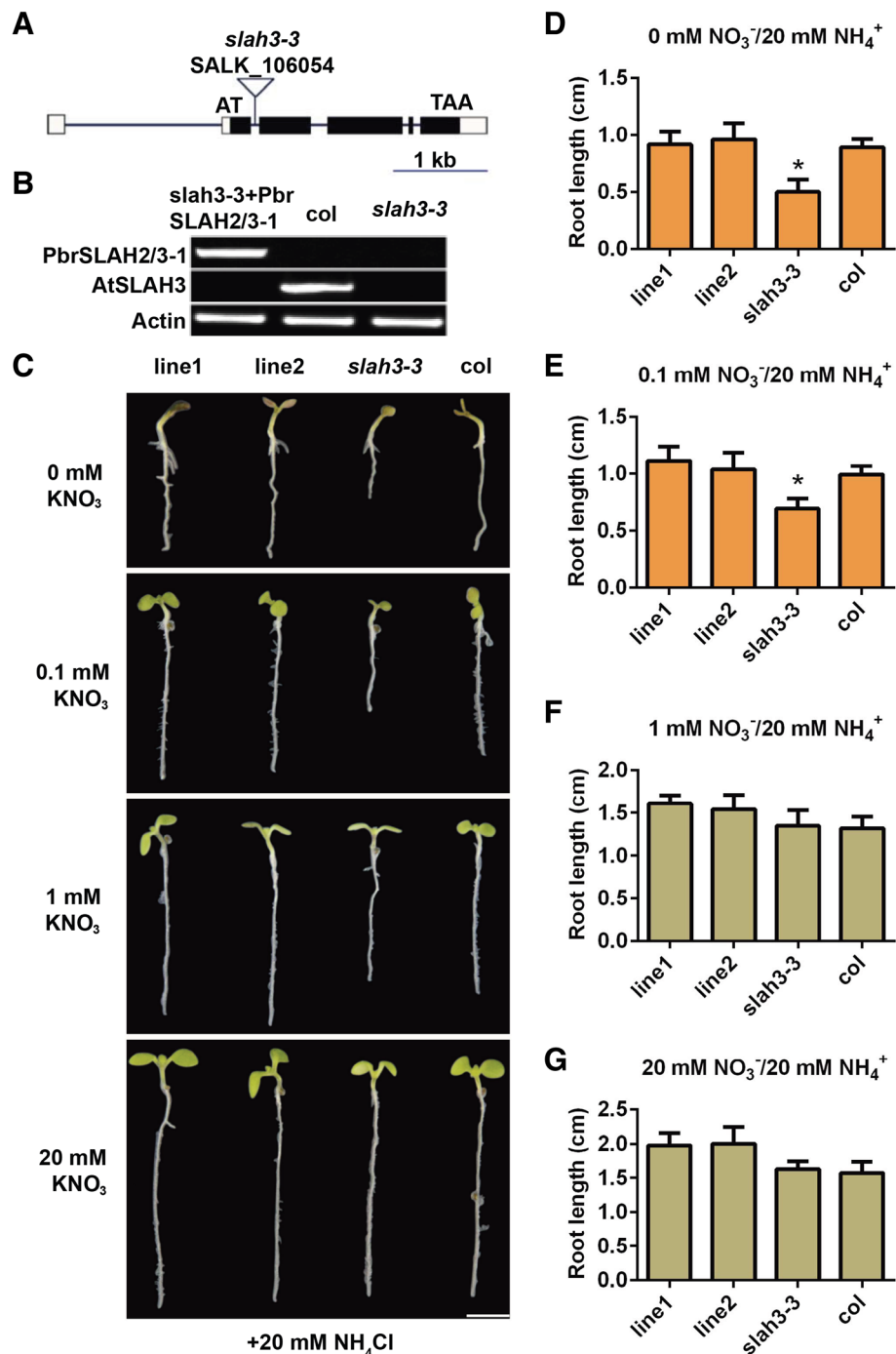


Fig. 3 PbrSLAH3 rescues the ammonium toxicity of *slah3-3* mutant plants under high ammonium/low-nitrate conditions. **a** Schematic map of the T-DNA insertion site in the *slah3-3* mutant. **b** RT-PCR analyses of *PbrSLAH3* and *AtSLAH3* expression levels in transgenic, wild-type (Col-0) and *slah3-3* mutant plants. Actin was used as a control. **c** Growth comparison among 7-d-old transgenic lines 1 and 2, wild-type (Col-0) and *slah3-3* mutant seedlings grown on 1/2 N-free Murashige and Skoog medium supplemented with different concentrations of KNO₃ (0–20 mM) and 20 mM NH₄Cl. **d–g** The average primary root lengths of seedlings under the same conditions as displayed in (c) were statistical analyzed. Results are averages ± SEs of three independent experiments (*n* = 15 per experiment). The asterisk represents statistical significance among transgenic lines, wild-type and *slah3-3* mutant plant (Student's *t*-test, **P* < 0.05). Bar = 0.5 cm

Identification of *PbrSLAH3* regulators

Considering the activation of the *AtSLAH3*-encoded channel requires the protein kinase *AtCPK21* [10, 13], and *PbrSLAH3* shows high similarity and similar function to that of *AtSLAH3*, we investigated whether *PbrSLAH3* can interact with *AtCPK21* to transport nitrate ions. BiFC assays showed that *PbrSLAH3* can interact with *AtCPK21* in the plasma membrane of tobacco epidermal cells (Additional file 1: Figure S3), indicating that *PbrSLAH3* may be involved in a signal-transduction pathway through phosphorylation and it may be a counterpart of *AtSLAH3*.

Given *PbrSLAH3* is activated by *AtCPK21*, we hypothesized that *PbrSLAH3* may be regulated by orthologs of *AtCPK21* in pear. We initially constructed a phylogenetic tree based on DNA sequences in pear to analyze associations between *PbrSLAH3* and CPKs owing to the characteristic interactions between CPKs and anion channel proteins in *Arabidopsis* (Additional file 1: Figure S4 and Table S2). We identified 17 candidate *PbrCPK* proteins that may interact with *PbrSLAH3* in pear. Then, a yeast two-hybrid experiment was firstly performed to assess the ability of *PbrSLAH3* to interact with each of the *PbrCPKs*. The full-length of *PbrSLAH3* fused with the pDHB-C and the *PbrCPKs* fused with the pPR3-N vector were then co-transformed into the yeast strain NMY51 using the lithium acetate method, respectively. Co-transformed yeast cells were first selected on plates containing medium lacking Trp and Leu to confirm the introduction of the *PbrSLAH3*-pDHB-C and *PbrCPKs*-pPR3-N plasmids into the yeast cells (Additional file 1: Figure S5). The positive clones were then transferred to selective plates lacking Trp, Leu, His and Ade. As shown in Additional file 1: Figure S5, yeast cells co-transformed with the positive controls (NubG and pDHB-C) and interactive genes (*PbrSLAH3*-pDHB-C and *PbrCPK32*-pPR3-N) could grow on the selective medium (SD/-Trp-Leu-His-Ade). However, yeast cells harboring *PbrSLAH3*-pDHB-C and the other *PbrCPKs*-pPR3-N plasmids could not grow on the selective media. To further confirm the interaction between *PbrSLAH3* and *PbrCPK32*, control experiments were performed to rule out self-activation. As shown in Fig. 4a, neither yeast cells harboring *PbrSLAH3*-pDHB-C and pPR3-N nor pDHB-C and *PbrCPK32*-pPR3-N could grow on the selective media. Only *PbrSLAH3*-pDHB-C and *PbrCPK32*-pPR3-N together could grow on the selective media (SD/-Trp-Leu-His-Ade; Fig. 4a). In addition, *PbrCPK32* is mainly expressed in the root system, and the subcellular localization study displayed that the *PbrCPK32*-GFP fusion protein is mostly distributed in the cell membrane (Additional file 1: Figure S6). In all, these results revealed that *PbrSLAH3* could interact with *PbrCPK32* in the plasma membrane.

To further confirm the interaction between *PbrSLAH3* and *PbrCPK32* in vivo, BiFC assays was performed (Fig. 4b). *PbrSLAH3* tagged with a split YFP^N-terminal fragment (nYFP) and *PbrCPK32* tagged with an YFP^C-terminal fragment (cYFP) were transiently co-infiltrated into epidermal cells of *N. benthamiana* leaves using *Agrobacterium*. As indicated in Fig. 4b, a strong YFP fluorescent signal was detected in the plasma membrane of epidermal cells when co-expression of *PbrSLAH3*-YFP^N and *PbrCPK32*-YFP^C or expression 35S-YFP alone (as a positive control), while no YFP fluorescent signal was observed in cells co-expressing of *PbrSLAH3*-YFP^N and YFP^C or *PbrCPK32*-YFP^C and YFP^N (Additional file 1: Figure S7). Thus, the BiFC assays further confirmed the interaction between *PbrSLAH3* and *PbrCPK32* in the plasma membrane.

PbrSLAH3 mediates S-type anion currents when co-expressed with CPKs in *Xenopus* oocytes

Since *AtCPK21* interacts with *PbrSLAH3*, we further tested whether this protein kinase regulates the activity of *PbrSLAH3*. When this putative anion channel was expressed alone in *Xenopus* oocytes, no YFP fluorescence signal was detected and no anion currents could be measured (Fig. 5a and Additional file 1: Figure S8). However, when *PbrSLAH3* was co-expressed with *AtCPK21*, YFP fluorescence was emitted from oocytes and typical anion currents were recorded in the presence of NO₃⁻ with membrane polarization (Fig. 5a).

In line with the functional characteristics of *AtSLAH3*, which is a preferential NO₃⁻-permeable channel that is 20 times more permeable to NO₃⁻ than Cl⁻, *PbrSLAH3* is also a preferential NO₃⁻-permeable channel. The magnitudes of the anion currents were greater in the nitrate-bath medium than that under the same concentration of chlorine. In addition, the anion currents were largely dependent on the extracellular NO₃⁻ concentrations (Fig. 5b). As shown in Fig. 5c, typical anion currents were elicited from oocytes in the presence of 25 mM nitrate medium. Although they were rather low, the anion currents increased 133 and 266% when the NO₃⁻ concentration reached up to 50 mM and 100 mM, respectively. Together, in the presence of extracellular nitrate solution, *PbrSLAH3* mediates S-type anion currents when co-expressed with *AtCPK21* in *Xenopus* oocytes.

Due to *PbrSLAH3* was activated by *AtCPK21* and an interaction was observed between *PbrSLAH3* and *PbrCPK32*, we hypothesized that the activity of *PbrSLAH3* was regulated by *PbrCPKs* in pear. To test this hypothesis, *PbrSLAH3* was injected alone or coinjected with *PbrCPK32* in the *Xenopus* oocytes. *PbrSLAH3* injected alone could not mediate the anion currents and no specific YFP fluorescence was emitted from *Xenopus* oocytes.

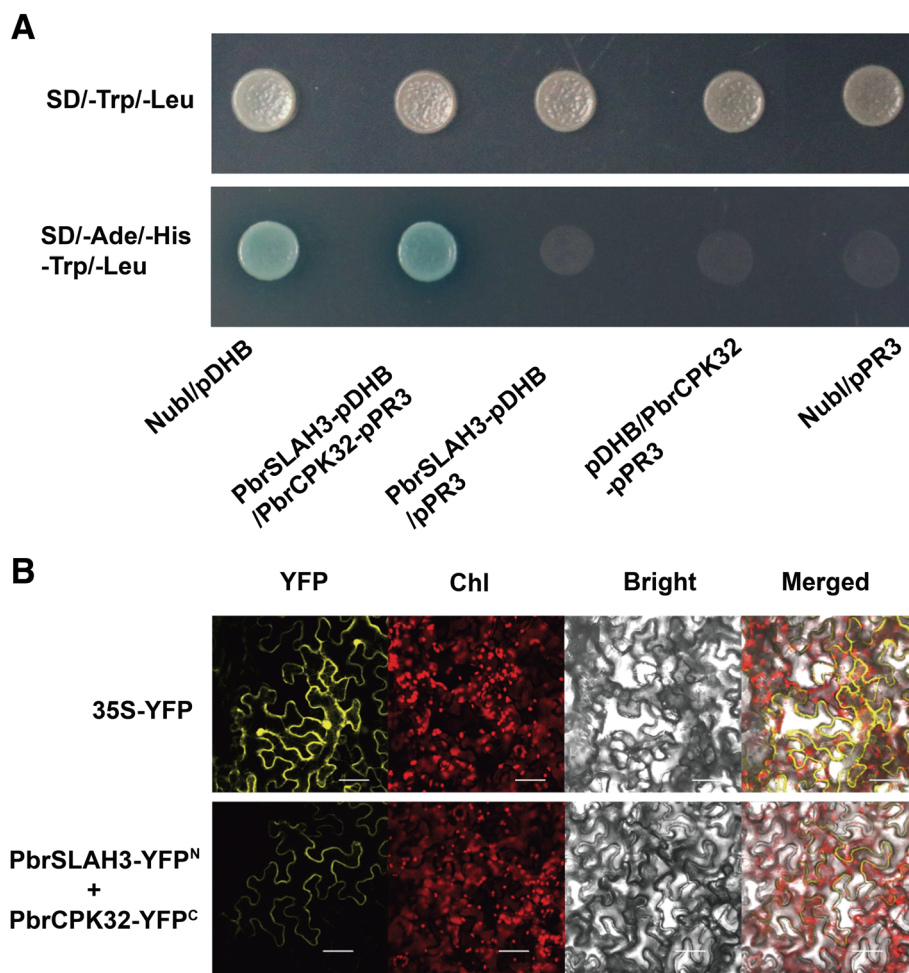


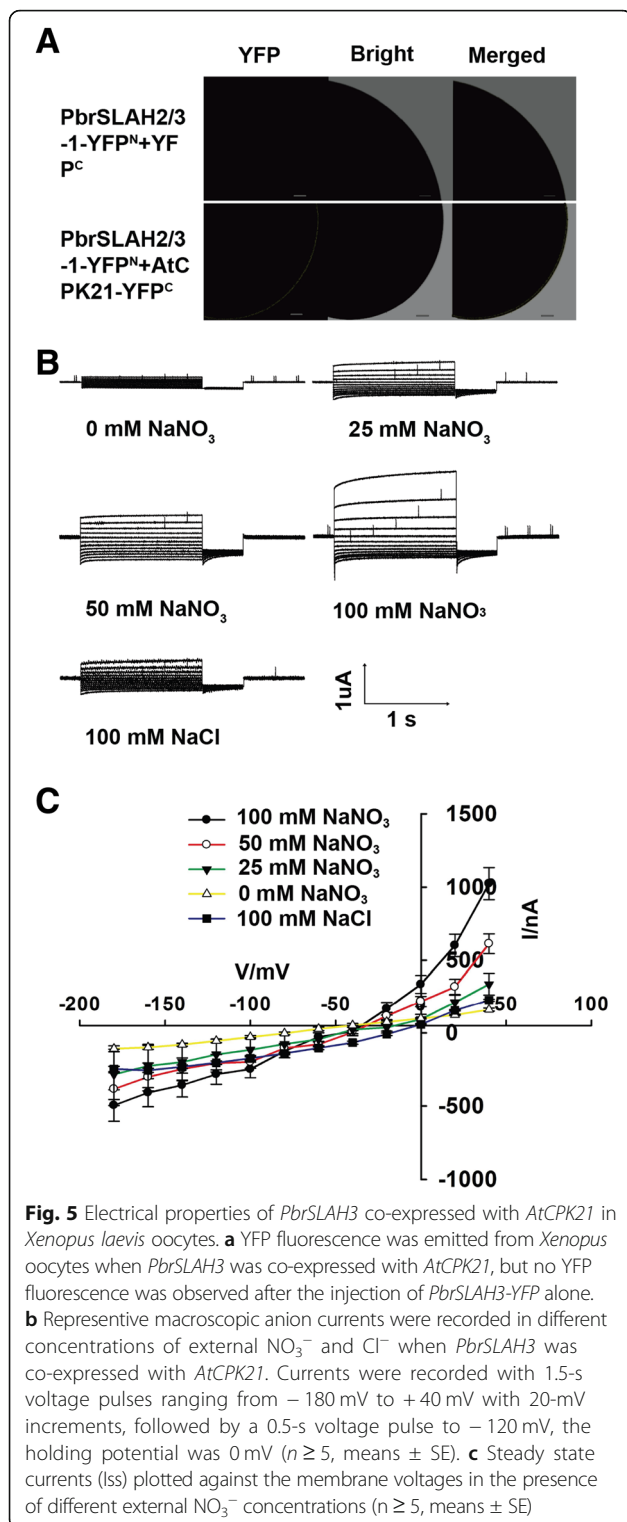
Fig. 4 Interaction between PbrSLAH3 and PbrCPK32 as assessed by yeast two-hybrid and bimolecular fluorescence complementation assays. **a** Yeast strain NMY51 co-transformed with the *PbrSLAH3* bait vector and *PbrCPK32* prey vector, along with a positive control (co-transformed Nubl vector and pDHB vector) were grown in medium lacking Ade, His, Trp and Leu. The negative control could not grow in the same medium. **b** YFP indicates yellow fluorescence protein; Chl: chlorophyll; Bright: bright-field image of *Nicotiana benthamiana* leaves infiltrated with *Agrobacterium tumefaciens*; Merge: digital merge of bright field and fluorescent images. Bar = 10 μ m

(Fig. 6a and Additional file 1: Figure S8). However, a YFP fluorescence signal was detected with a laser microscope (Fig. 6a) and macroscopic currents were elicited in the *Xenopus* oocytes when co-expression the *PbrSLAH3* with *PbrCPK32* (Fig. 6b). The I–V curves plotted against different concentrations of NO_3^- showed that the magnitudes of the anion currents mediated by PbrSLAH3 were strongly dependent on the external NO_3^- concentrations. However, only small macroscopic currents were induced by extracellular Cl^- . Furthermore, the rate of NO_3^- decrements was higher for 35S:*PbrSLAH3* plants than that of the *slah3-3* mutant *Arabidopsis*, based on NO_3^- measurements from culture solution (Additional file 1: Figure S9). However, the rate of Cl^- decrements was barely changed between 35S:*PbrSLAH3* plants and *slah3-3* mutant *Arabidopsis*, based on Cl^- measurements from culture solution (Additional file 1: Figure S9), which indicated that

overexpression of *PbrSLAH3* was greatly permeable NO_3^- than Cl^- in the root. Taken together these results demonstrated that PbrSLAH3 was activated by PbrCPK32 and exhibited highly nitrate selectivity without obvious permeability to chloridion.

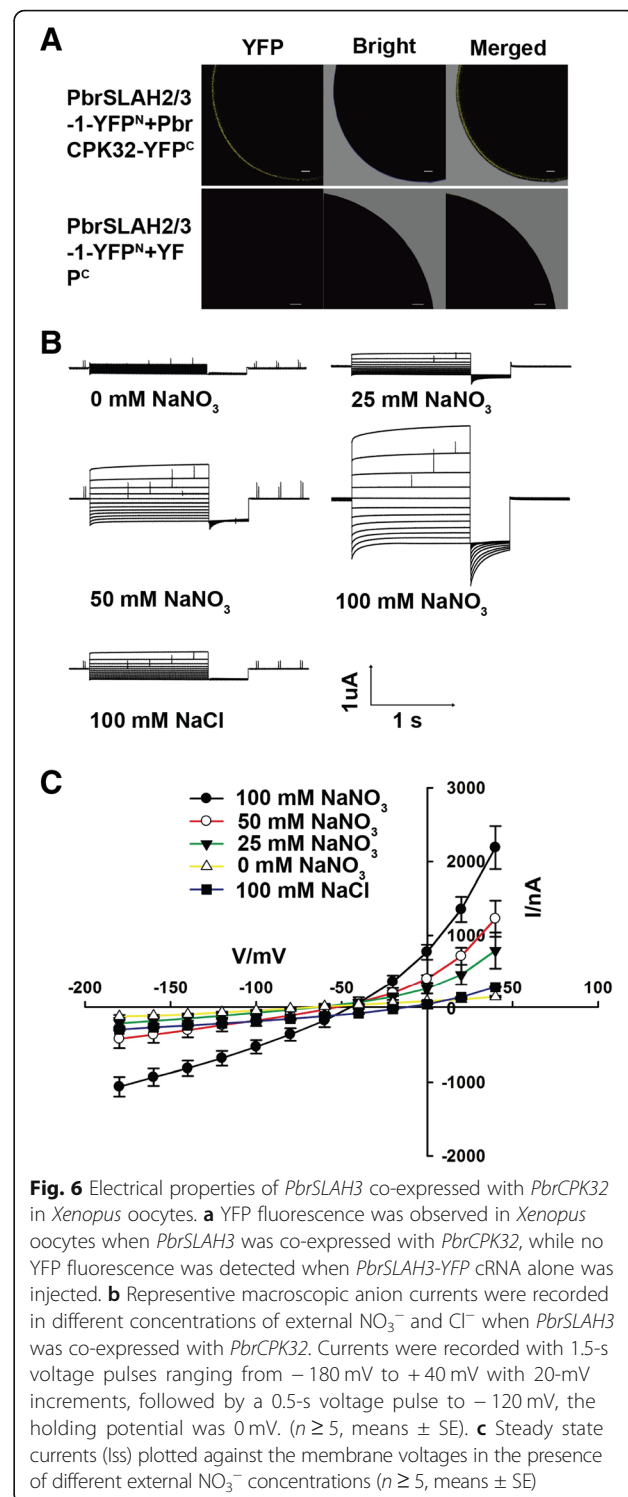
Discussion

Nitrate is an important nutrient, and is also widely used as a signaling molecule during plant growth and development [14]. Following the up-take of nitrate by plasma membrane-localized nitrate transporters, nitrate is translocated into the vasculature for long-distance transport. It has been reported that *SLAC/SLAH* family genes could mediate the NO_3^- efflux and may participate in NO_3^- transport [20, 22, 25]. Considering *AtSLAC1* is exclusively expressed in guard cells, the other four *AtSLAH* (*SLAH1* to *SLAH4*) genes, which are predominantly



expressed in root, are targets for NO_3^- translocation in *Arabidopsis* root or from the root to shoot.

Based on previous reports about *SLAC/SLAH* genes expression patterns and functional characteristics [12, 28], we hypothesized that some members of



the *SLAC/SLAH* family in pear may be involved in nitrate transport in root or from the root to the shoot, and may play an important role in determining the nitrogen use efficiency of the pear. In this study, four putative *SLAC/SLAH* genes were identified in the *Pyrus* genome. Surprisingly, it was found

that orthologs of *AtSLAC/SLAH* in pear did not phylogenetically cluster with *AtSLAH1* and *AtSLAH4*. While, the expression patterns of *PbrSLAC/SLAH* are consistent with previous reports [25], *PbrSLAC1* is strongly expressed in leaves, and *PbrSLAH3* displays a higher expression level than other *SLAH* genes in pear root. Therefore, we presumed that *PbrSLAH3* may predominantly participate in NO_3^- transport in pear root. Here, the functional characteristics of *PbrSLAH3* were mainly studied using complementation lines and a *Xenopus* oocyte heterogeneous expression system.

The predominant expression of *PbrSLAH3* in root was further confirmed by RT-PCR and GUS staining assays, which demonstrated that it was also expressed in guard cells and pollen tubes, suggesting that *PbrSLAH3* may have diverse functions similar to those of *AtSLAH3*. Furthermore, phenotype assays showed that *PbrSLAH3* also rescues the ammonium toxicity phenomenon of the *slah3-3* mutant under low NO_3^- /high NH_4^+ conditions similar to that of the *AtSLAH3*. Taken together, we presumed that *PbrSLAH3* together with *AtSLAH3* and other orthologes from different species may be used as promising targets for crop enhancement, and they may serve as potential targets for transgenic breeding approaches to improve nitrogen use efficiency and reduce dependency on nitrogen fertilizers.

Post-translational modifications of transport proteins play key roles in the regulation of anion transport activities. For instance, *AtSLAC1* and *AtSLAH3* were activated by the Ca^{2+} -independent protein kinase OST1 [29–31], as well as by *AtCPKs* [24, 29, 32]. *SLAH2* was activated by *CPK21* and *CIPK23* kinases [22]. In this study, *PbrSLAH3* was confirmed to interact with *PbrCPK32* through yeast two-hybrid and BiFC assays. Furthermore, the electrophysiological experiments demonstrated that *PbrSLAH3*'s activation requires phosphorylation. When *PbrSLAH3* alone injection into *Xenopus* oocytes, no currents were elicited, but when *PbrSLAH3* and *AtCPK21* were co-expressed in the *Xenopus* oocytes, typical anion currents were recorded in the presence of NO_3^- . However, not all isolated anion channels from different species dependent on the phosphorylation process. For example, *PttSLAH3* isolated from poplar is activated independent of phosphorylation by protein kinases [10]. In addition, the silent *SLAH1* subunit gates *SLAH3* open even in the absence of calcium-dependent kinases when co-expression the *SLAH1* and *SLAH3* in *Xenopus* oocytes [20]. In line with the function characteristic of the *AtSLAH3*, *PbrSLAH3* was strongly dependent on the external concentration of NO_3^- and showed a high selectivity for nitrate over chloride. However, the biological functions of *PbrSLAH3* and *PbrCPK32* in pear are still unknown.

Conclusions

S-type anion channels play an important role in nitrate translocation, revealing another manner to expand the transport of nitrate anions. However, the function characteristics of *PbrSLAC/SLAH* in pear have not been clarified. In this study, four members of S-type anion channels were identified in pear using *Arabidopsis SLAC/SLAH* sequences as queries. In combination with homologous similarity and expression analyses, *PbrSLAH3* was selected as a candidate gene involved in NO_3^- transport in pear root. The physiological function of *PbrSLAH3* was investigated by complementation lines, growth assays suggested that *PbrSLAH3* participates in the alleviation of ammonium toxicity. *PbrSLAH3* interaction with *PbrCPK32* was firstly confirmed by yeast two-hybrid and BiFC assays, and *PbrSLAH3* activity was controlled through phosphorylation by *CPKs* was further verified by co-expression it with *AtCPK21* or *PbrCPK32* in *Xenopus* oocytes. Furthermore, electrophysiological and physiology experiment results showed that *PbrSLAH3* was more permeable to NO_3^- than Cl^- . Taken together these results, we concluded that *PbrSLAH3* crossing-talk with *PbrCPK32* may participate in transporting NO_3^- in pear root.

Methods

Plant materials and growth conditions

The Columbia (Col-0) line of *Arabidopsis* was used as the wild-type (Col-0). The *slah3-3* (SALK_106054) mutant seed was ordered from the *Arabidopsis* Biological Resource Center. Homozygous mutant plants were isolated by PCR with corresponding primers, as listed in Additional file 1: Table S1. For seed harvest, *Arabidopsis* plants were grown in a potting soil mixture (rich soil:vermiculite = 2:1, v/v) and kept in growth chambers with a light/dark regime of 14/10 h, at 28/22 °C with 75% relative humidity and a light intensity of $800 \mu\text{mol m}^{-2} \text{s}^{-1}$. For nitrate treatment experiments, surface-sterilized seeds were germinated and grown on 1/2 N-free Murashige and Skoog medium (pH 5.8) containing different concentrations (0–20 mM) of KNO_3 with or without 20 mM ammonium chloride. Plates were kept at 4 °C for 3 d before seed germination. All plants were grown vertically under axenic conditions in growth chambers as described above. Plants were photographed with a Canon EOS 80D camera (Canon, Tokyo, Japan). Statistical analyses of the data were performed using the SPSS statistical package (SPSS Version 17.0 for Windows; SPSS Inc., Chicago, IL).

Bioinformatics analysis of *PbrSLAC/PbrSLAH*

The protein sequences of *AtSLAC1* (AT1G12480), *AtSLAH1* (AT1G62280), *AtSLAH2* (AT4G27970), *AtSLAH3* (AT5G24030) and *AtSLAH4* (AT1G62262) were used as queries to perform a BLAST algorithm-based

search of the pear genome database (<http://peargenome.njau.edu.cn/>). Based on our previous research, four PbrSLAC/SLAH protein sequences were identified [33]. They were aligned with orthologs in *Arabidopsis*, and a phylogenetic tree was generated by MEGA (version 6.0) software with the neighbor-joining method and a bootstrap test of 1000 replicates [34].

RNA isolation and qRT-PCR assays

Total RNA was extracted from different parts (root, stem, leaf, flower, fruit, pollen grain and pollen tube) of pear using an RNA extracting kit (RNAsimply Total RNA Kit, Tiangen, Beijing, China) according to the manufacturer's protocol. Then approximately 2 µg total RNA was used for first-strand cDNA synthesis using TransScript[®]One-Step gDNA Removal and cDNA Synthesis SuperMix (TRANSGEN, Beijing, China). Three biological and three technical replicates were processed for the qRT-PCR assays, which was performed in 20 µL reaction mixture containing 80–100 ng cDNA, 200 nM of each primer (Additional file 1: Table S1) and 10 µL LightCycler 480 SYBRGREEN I Master Mix (Roche, Basel, Switzerland). All reactions were carried out in a CFX96 Real-Time System (Roche), following a three step standard protocol (45 cycles of 10 s at 95 °C, 30 s at 60 °C and 30 s at 72 °C), followed by a melt curve analysis. The expression levels of *PbrSLAC/SLAH* genes were calibrated by the $2^{-\Delta\Delta C_t}$ method using *PbrUBQ* and *PbrTUB* as reference genes [35]. RT-PCR was carried out on a Veriti[™] 96-Well Thermal cycler (Bio-Rad, Richmond, CA, USA) using Taq DNA Polymerase (New England Biolabs, Beverly, MA, USA). *PbrUBQ* was used as the reference gene. PCR products were separated on a 2% (w/v) agarose gel stained with ethidium bromide.

Subcellular localization assays

To test the subcellular localization of PbrSLAH3 and its regulatory protein, the full-length coding sequences of *PbrSLAH3* and *PbrCPK32* were amplified with the corresponding primers, respectively, which are listed in Additional file 1: Table S1. The purified PCR products were independently inserted into the pCAMBIA1302 vector under the control of the CaMV 35S promoter and the vector is detailed in xie et al [36]. The recombinant plasmids 35S:*PbrSLAH3*-green fluorescence protein (GFP) and 35S:*PbrCPK32*-GFP, as well as the control plasmid 35S:GFP, were independently introduced into *Nicotiana benthamiana* leaves by *Agrobacterium*-mediated transformation. Transformed leaves were stained with double-distilled water supplemented with 5 µM FM4–64 (Invitrogen) for 15 min, and the GFP signal was detected with a Zeiss LSM 780 Image Browser (Carl Zeiss Inc.) 3 d after transformation.

BiFC assays

The full-length cDNAs of *PbrSLAH3* and *PbrCPK32* were each inserted independently into the pYFP-N and pYFP-C vectors [37] and sequenced. Then, *N. benthamiana* leaves were transiently transformed using the *Agrobacterium* infection method with different combinations of these vectors. After 3 d, the YFP expression signals emitted from *N. benthamiana* leaves were observed with a Zeiss LSM 780 Image Browser (Carl Zeiss Inc.).

Yeast two-hybrid assays

To screen for interactions between PbrSLAH3 and PbrCPKs, the coding sequence of *PbrSLAH3* was cloned into the pDHB-C vector, and the full-length *PbrCPK* cDNAs were independently cloned into the pPR3-N vector [38]. Next, *PbrSLAH3*-pDHB-C and *PbrCPK*-pPR3-N plasmids were co-transformed into the yeast strain NMY51 using the lithium acetate method. NubG co-transformed with pDHB-C was used as a positive control, and NubG co-transformed with pPR3-N was used as a negative control. Then, co-transformed yeast cells were grown on selective medium lacking leucine and tryptophan (SD/-Trp-Leu) and were cultured at 28 °C. Colonies from SD/-Trp-Leu plates were transferred to plates lacking leucine, tryptophan, histidine and adenine (SD/-Trp-Leu-His-Ade) and dyed with X-gal to test for possible interactions.

Vector construction and *Arabidopsis* transformation

The *PbrSLAH3* promoter fragment (~ 2 kb) was cloned into the pBasta-GUSGW vector [39], and *PbrSLAH3* was cloned into the pCAMBIA1302 vector [36]. Then, *PbrSLAH3*::GUS and *PbrSLAH3*-pCAMBIA1302 recombination vectors were transformed into Col-0 *Arabidopsis* plants and *slah3* mutant plants, respectively. The *Arabidopsis* transformation was performed using the floral dip method with *Agrobacterium* GV3101 [40]. The seeds of the transgenic plants were collected and then plated on half-strength MS medium containing 30 mg/L of hygromycin. Positive seedlings were verified by PCR with primers listed in Additional file 1: Table S1, and T3 homozygous transgenic lines were used for the later GUS assays and phenotypic analysis.

GUS assays

GUS staining was carried out according to the method described by Jefferson et al [40, 41]. Two-week-old seedlings, flowers and siliques were vacuum-infiltrated for 30 min in the staining solution (GUS staining kit, Pulangtai, Beijing, China) followed by incubation at 37 °C for 3 h. After gradient decolorization by alcohol, the samples were photographed under a microscope with a Canon EOS 80D camera (Canon, Tokyo, Japan).

Double-electrode voltage-clamp studies (oocyte recordings)

PbrSLAH3 cDNA fused with pYFP-C and *PbrCPK32* cDNA fused with pYFP-N were independently cloned into the pT7TS vector using homologous recombination technology [42]. The capped and polyadenylated cRNA of these two fusion genes were synthesized in vitro using a MESSAGE kit (Ambion, Austin, Texas, USA). Then, 50 nL cRNA mixture of the target genes (*PbrSLAH3*-YFP-C and *PbrCPK32*-YFP-N) or 50 nL of deionized water (control) was injected into matured oocytes, which were then cultured in 'ND96' solution (96 mM NaCl, 2 mM KCl, 1.8 mM CaCl₂, 1 mM MgCl₂ and 5 mM HEPES, adjusted to pH 7.4 with NaOH) until electrophysiological recordings were taken. Then, 3–5 d after cRNA injections, whole-oocyte currents were recorded using the two-electrode voltage-clamp technique. The voltage-clamp amplifier was an Axoclamp 900A (Axon Instruments, Foster City, CA, USA). Electrodes were filled with 3 M KCl, and the standard solution contained 5 mM Tris/MES (pH 7.5), 1 mM Ca(gluconate)₂, 1 mM Mg(gluconate)₂, 100 mM NaNO₃ and 1 mM LaCl₃. To balance the ionic strength, nitrate or chloride variations were compensated with sorbitol. Osmolality was adjusted to 220 mosmol/kg with D-sorbitol. The voltage-clamp protocols are described in the figure legends, and data acquisition and data analyses were performed using pClampfit 10.3 (Molecular Devices) and Sigmaplot 12.5 software (Jandel Scientific, Erkrath, Germany), respectively. Absorption or transport.

Determination of the NO₃⁻ and Cl⁻ contents

The 35S:*PbrSLAH3* and *slah3-3* mutant *Arabidopsis* seeds were plated on solid 1/2 MS medium. Two-week-old seedlings were pre-cultured in the 72 holes rectangular box containing 500 mL of liquid 1/2 MS medium for 12 d. In the process of pre-culture, the nutrient solution was replaced with fresh solution every 4 d. After the pre-culture, seedlings were treated with the 1/2 NO₃⁻-free and Cl⁻-free MS for 3 days, and then were transferred into modified liquid 1/2 MS containing 5 mM NO₃⁻ and 5 mM Cl⁻. 180 seedlings were used per treatment, with three replications. Concentrations of NO₃⁻ and Cl⁻ were determined in the liquid 1/2 MS solution at 0 h, 6 h, 12 h, 24 h, 48 h and 96 h after the transferring, respectively, which are based on the method described by Cataldo et al [43] and Gilliam et al [44]. In addition, the volume of nutrient solution needs to be replenished to 500 mL with double distilled water before each sampling. Statistical analyses of the data were performed using the SPSS statistical package (SPSS Version 17.0 for Windows; SPSS Inc., Chicago, IL). Three biological replicates and three technical replicates were processed, and all plants were grown in chambers with a light/dark regime of 14/10 h, at 28/22 °C with 75% relative humidity and a light intensity of 800 μmol m⁻² s⁻¹.

Additional file

Additional file 1: Figure S1. Changes in PbrSLAH3 expression in response to re-supplying nitrate in pear root after nitrate starvation. **Figure S2.** PbrSLAH3 rescues the ammonium toxicity of *slah3-3* mutant plants under high-ammonium/low-nitrate conditions. **Figure S3.** PbrSLAH3 interaction with AtCPK21 was confirmed by bimolecular fluorescence complementation assays. **Figure S4.** Phylogenetic tree of calcium-dependent proteins in pear and in *Arabidopsis*. **Figure S5.** The interaction between *PbrSLAH3* and *PbrCPKs* was assessed by the yeast two-hybrid assays. **Figure S6.** The subcellular localization of *PbrCPK32* in plasma membrane and the expression profiles of the *PbrCPK32* genes in different parts of the pear were analyzed by qRT-PCR. **Figure S7.** No fluorescence was detected when *PbrSLAH3* or *PbrCPK32* was expressed alone in *N. benthamiana* leaves (negative control). **Figure S8.** Representative macroscopic anion currents were recorded in 50 mM NaNO₃ solution after independently injects of H₂O and PbrSLAH₃ alone. **Figure S9.** Comparative analysis of NO₃ and Cl transport between 35S:*PbrSLAH3* and *slah3-3* mutant plants. **Table S1.** Primers used in this study. **Table S2.** CPK family genes identified in pear. (PDF 1355 kb)

Abbreviations

ABA: Abscisic acid; Ade: Adenine; BiFC: Bimolecular fluorescence complementation; CPK: Calcium-dependent protein kinase; GFP: Green Fluorescent Protein; GUS: β-Glucuronidase; His: Leucine; Leu: Leucine; OST1: Stomatal opening factor 1; qRT-PCR: Quantitative real-time polymerase chain reaction; RT-PCR: Real-time polymerase chain reaction; S-type anion channels: S-type anion channels; Trp: Tryptophan; YFP: Yellow Fluorescent Protein

Acknowledgements

Not applicable.

Funding

The National Key R&D Program of China (2018YFD0201400) and the National Key Technology R&D Program of the Ministry of Science and Technology of China (2014BAD16B03–4) were supported for designing the study and carrying out the experiments, the Fundamental Research Funds for the Central Universities (KJQN201926 and KYTZ201602) was supported for analysis and interpretation of data, and the National Natural Science Foundation of China (31801842) was supported for polish the manuscript.

Availability of data and materials

The data and material that support the findings of this study are available from the corresponding author on request.

Authors' contributions

CGD designed the research, performed the experiments, and analyzed the results. WL and WJY drafted the manuscript. CQ, CP, TC and WX participated in carrying out the experiments. WJY, WL, QKJ, YH, ZSL, and WP participated in revising the final manuscript. WJY managed the experiments. All authors have read and approved the final manuscript.

Ethics approval and consent to participate

Not applicable.

Consent for publication

Not applicable.

Competing interests

The authors declare that they have no competing interests.

Publisher's Note

Springer Nature remains neutral with regard to jurisdictional claims in published maps and institutional affiliations.

Received: 17 August 2018 Accepted: 30 April 2019
Published online: 08 May 2019

References

- Zimmermann S, Ehrhardt T, Plesch G, Müller-Rober B. Ion channels in plant signaling. *Cell Mol Life Sci*. 1999;55(2):183–203.
- Czempinski K, Gaedeke N, Zimmermann S, Müller-Rober B. Molecular mechanisms and regulation of plant ion channels. *J Exp Bot*. 1999;50:955–66.
- Blatt MR, Thiel G. Hormonal-control of Ion-Channel gating. *Annu Rev Plant Phys*. 1993;44:543–67.
- Tyerman SD. Anion channels in plants. *Annu Rev Plant Phys*. 1992;43:351–73.
- Neher E, Sakmann B. The patch clamp technique. *Sci Am*. 1992;266(3):44–51.
- Keller BU, Hedrich R, Raschke K. Voltage-dependent anion channels in the plasma-membrane of guard-cells. *Nature*. 1989;341(6241):450–3.
- Schroeder JJ, Hagiwara S. Cytosolic calcium regulates ion channels in the plasma-membrane of *Vicia-Faba* guard-cells. *Nature*. 1989;338(6214):427–30.
- Vahisalu T, Kollist H, Wang YF, Nishimura N, Chan WY, Valerio G, Lamminmaki A, Brosche M, Moldau H, Desikan R, et al. SLAC1 is required for plant guard cell S-type anion channel function in stomatal signalling. *Nature*. 2008;452(7186):487–91.
- Negi J, Matsuda O, Nagasawa T, Oba Y, Takahashi H, Kawai-Yamada M, Uchimiya H, Hashimoto M, Iba K. CO₂ regulator SLAC1 and its homologues are essential for anion homeostasis in plant cells. *Nature*. 2008;452(7186):483–U413.
- Jaborsky M, Maierhofer T, Olbrich A, Escalante-Perez M, Müller HM, Simon J, Krol E, Cui TA, Fromm J, Ache P, et al. SLAH3-type anion channel expressed in poplar secretory epithelia operates in calcium kinase CPK-autonomous manner. *New Phytol*. 2016;210(3):922–33.
- Sun SJ, Qi GN, Gao QF, Wang HQ, Yao FY, Hussain J, Wang YF. Protein kinase OsSAPK8 functions as an essential activator of S-type anion channel OsSLAC1, which is nitrate-selective in rice. *Planta*. 2016;243(2):489–500.
- Geiger D, Scherzer S, Mumm P, Stange A, Marten I, Bauer H, Ache P, Matschi S, Liese A, Al-Rasheid KA, et al. Activity of guard cell anion channel SLAC1 is controlled by drought-stress signaling kinase-phosphatase pair. *Proc Natl Acad Sci U S A*. 2009;106(50):21425–30.
- Geiger D, Maierhofer T, Al-Rasheid KAS, Scherzer S, Mumm P, Liese A, Ache P, Wellmann C, Marten I, Grill E, et al. Stomatal closure by fast abscisic acid signaling is mediated by the guard cell anion channel SLAH3 and the receptor RCAR1. *Sci Signal*. 2011;4(173):ra32.
- Wang YY, Hsu PK, Tsay YF. Uptake, allocation and signaling of nitrate. *Trends Plant Sci*. 2012;17(8):458–67.
- Dreyer I, Gomez-Porras JL, Riano-Pachon DM, Hedrich R, Geiger D. Molecular evolution of slow and quick anion channels (SLACs and QUACs/ALMTs). *Front Plant Sci*. 2012;3:263.
- Desikan R, Griffiths R, Hancock J, Neill S. A new role for an old enzyme: nitrate reductase-mediated nitric oxide generation is required for abscisic acid-induced stomatal closure in *Arabidopsis thaliana*. *Proc Natl Acad Sci U S A*. 2002;99(25):16314–8.
- Yoshida R, Umezawa T, Mizoguchi T, Takahashi S, Takahashi F, Shinozaki K. The regulatory domain of SRK2E/OST1/SnRK2.6 interacts with ABI1 and integrates abscisic acid (ABA) and osmotic stress signals controlling stomatal closure in *Arabidopsis*. *J Biol Chem*. 2006;281(8):5310–8.
- Chen YH, Hu L, Punta M, Bruni R, Hillerich B, Kloss B, Rost B, Love J, Siegelbaum SA, Hendrickson WA. Homologue structure of the SLAC1 anion channel for closing stomata in leaves. *Nature*. 2010;467(7319):1074–80.
- Demir F, Horntrich C, Blachutzik JO, Scherzer S, Reinders Y, Kierszniowska S, Schulze WX, Harms GS, Hedrich R, Geiger D, et al. *Arabidopsis* nanodomain-delimited ABA signaling pathway regulates the anion channel SLAH3. *Proc Natl Acad Sci U S A*. 2013;110(20):8296–301.
- Cubero-Font P, Maierhofer T, Jaslan J, Rosales MA, Espartero J, Diaz-Rueda P, Müller HM, Hurter AL, Al-Rasheid KAS, Marten I, et al. Silent S-type anion channel subunit SLAH1 gates SLAH3 open for chloride root-to-shoot translocation. *Curr Biol*. 2016;26(16):2213–20.
- Qiu JE, Henderson SW, Tester M, Roy SJ, Gilliam M. SLAH1, a homologue of the slow type anion channel SLAC1, modulates shoot Cl⁻ accumulation and salt tolerance in *Arabidopsis thaliana*. *J Exp Bot*. 2016;67(15):4495–505.
- Maierhofer T, Lind C, Huttel S, Scherzer S, Papenfuss M, Simon J, Al-Rasheid KA, Ache P, Rennenberg H, Hedrich R, et al. A single-pore residue renders the *Arabidopsis* root anion channel SLAH2 highly nitrate selective. *Plant Cell*. 2014;26(6):2554–67.
- Winter D, Vinegar B, Nahal H, Ammar R, Wilson GV, Provart NJ. An "electronic fluorescent pictograph" browser for exploring and analyzing large-scale biological data sets. *PLoS One*. 2007;2(8):e718.
- Gutermuth T, Lässig R, Portes MT, Maierhofer T, Romeis T, Borst JW, Hedrich R, Feijo JA, Konrad KR. Pollen tube growth regulation by free anions depends on the interaction between the anion channel SLAH3 and calcium-dependent protein kinases CPK2 and CPK20. *Plant Cell*. 2013;25(11):4525–43.
- Zheng XJ, He K, Kleist T, Chen F, Luan S. Anion channel SLAH3 functions in nitrate-dependent alleviation of ammonium toxicity in *Arabidopsis*. *Plant Cell Environ*. 2015;38(3):474–86.
- Stitt M, Müller C, Matt P, Gibon Y, Carillo P, Morcuende R, Scheible WR, Krapp A. Steps towards an integrated view of nitrogen metabolism. *J Exp Bot*. 2002;53(370):959–70.
- Wolf-Rüdiger Scheible MS. Genome-wide reprogramming of primary and secondary metabolism, protein synthesis, cellular growth processes, and the regulatory infrastructure of *Arabidopsis* in response to nitrogen. *Plant Physiol*. 2004;136(1):2483–99.
- Park H, Oh SJ, Han KS, Woo DH, Park H, Mannaioni G, Traynelis SF, Lee CJ. Bestrophin-1 encodes for the Ca²⁺-activated anion channel in hippocampal astrocytes. *J Neurosci*. 2009;29(41):13063–73.
- Brandt B, Brodsky DE, Xue S, Negi J, Iba K, Kangasjarvi J, Ghasseman M, Stephan AB, Hu H, Schroeder JJ. Reconstitution of abscisic acid activation of SLAC1 anion channel by CPK6 and OST1 kinases and branched ABI1 PP2C phosphatase action. *Proc Natl Acad Sci U S A*. 2012;109(26):10593–8.
- Vahisalu T, Puzorjova I, Brosche M, Valk E, Lepiku M, Moldau H, Pechter P, Wang YS, Lindgren O, Salojarvi J, et al. Ozone-triggered rapid stomatal response involves the production of reactive oxygen species, and is controlled by SLAC1 and OST1. *Plant J*. 2010;62(3):442–53.
- Imes D, Mumm P, Bohm J, Al-Rasheid KAS, Marten I, Geiger D, Hedrich R. Open stomata 1 (OST1) kinase controls R-type anion channel QUAC1 in *Arabidopsis* guard cells. *Plant J*. 2013;74(3):372–82.
- Geiger D, Scherzer S, Mumm P, Marten I, Ache P, Matschi S, Liese A, Wellmann C, Al-Rasheid KA, Grill E, et al. Guard cell anion channel SLAC1 is regulated by CDPK protein kinases with distinct Ca²⁺ affinities. *Proc Natl Acad Sci U S A*. 2010;107(17):8023–8.
- Chen G. The slow anion channel (SLAC/SLAH) gene family in pear (*Pyrus bretschneideri*) and comparison with other members of the *Rosaceae*. *Genomics*. 2018. <https://doi.org/10.1016/j.ygeno.2018.07.004>.
- Tamura K, Dudley J, Nei M, Kumar S. MEGA4: molecular evolutionary genetics analysis (MEGA) software version 4.0. *Mol Biol Evol*. 2007;24(8):1596–9.
- Livak KJ, Schmittgen TD. Analysis of relative gene expression data using real-time quantitative PCR and the 2^{-ΔΔC_T} method. *Methods*. 2001;25(4):402–8.
- Xie QG, Wang P, Liu X, Yuan L, Wang LB, Zhang CG, Li Y, Xing HY, Zhi LY, Yue ZL, et al. LNK1 and LNK2 are transcriptional coactivators in the *Arabidopsis* circadian oscillator. *Plant Cell*. 2014;26(7):2843–57.
- Sun L, Song L, Zhang Y, Zheng Z, Liu D. *Arabidopsis* PHL2 and PHL1 act redundantly as the key components of the central regulatory system controlling transcriptional responses to phosphate starvation. *Plant Physiol*. 2016;170(1):499.
- Dong JS, Pinos MA, Li XX, Yang HB, Liu Y, Murphy AS, Kochian LV, Liu D. An *Arabidopsis* ABC transporter mediates phosphate deficiency-induced remodeling of root architecture by modulating iron homeostasis in roots. *Mol Plant*. 2017;10(2):244–59.
- Xie XB, Zhao J, Hao YJ, Fang CB, Wang Y. The ectopic expression of apple MYB1 and bHLH3 differentially activates anthocyanin biosynthesis in tobacco. *Plant Cell Tissue Org*. 2017;131(1):183–94.
- Clough SJ, Bent AF. Floral dip: a simplified method for *Agrobacterium*-mediated transformation of *Arabidopsis thaliana*. *Plant J*. 1998;16(6):735–43.
- Jefferson RA, Kavanagh TA, Bevan MW. GUS fusions β-glucuronidase as a sensitive and versatile gene fusion marker in higher-plants. *EMBO J*. 1987; 6(13):3901–7.
- Mei W, Song W, Pan Y, Gong W, Zhu Y. High throughput cloning of *Arabidopsis* transcription factors using gateway cloning technology. *Mol Plant Breed*. 2004;2(3):358–64.
- Cataldo D, Maroon M, Schrader L, Youngs V. Rapid colorimetric determination of nitrate in plant tissue by nitration of salicylic acid. *Commun Soil Sci Plan*. 1975;6(1):71–80.
- Gilliam JW. Rapid measurement of chlorine in plant materials. *Soil Sci Soc Am J*. 1971;35(3):512–3.